

# Many-Body Stochastic Dynamics: Quenches in Dissipative Quantum Spin Arrays

Loïc Henri<sup>1</sup> and Karyn Le Hur<sup>1</sup>

<sup>1</sup>*Centre de Physique Théorique, Ecole Polytechnique, CNRS, 91128 Palaiseau Cedex France*

(Dated: December 3, 2024)

We address dissipation effects on non-equilibrium properties of quantum spin arrays induced by quenches or Landau-Zener transitions. The dissipation is modeled by a bath of harmonic oscillators, here a ohmic bosonic bath. We develop a stochastic approach allowing to describe quantum quenches and interferometry in an exact manner beyond the “dissipative one-spin-1/2” limit. For two spins, the environment can also engender a dissipative quantum phase transition of Kosterlitz-Thouless type. In the case of a quantum Ising chain in a transverse field, we assume long-range interactions between spins and address the interplay between Landau-Zener-Stueckelberg-Majorana interferometry, many-body quenches, dissipative quantum phase transitions, and bath-engineering. We build a Kibble-Zurek type argument to account for non-equilibrium and interaction effects in the lattice. Such dissipative quantum spin arrays can be realized in ultra-cold atom, trapped ion and mesoscopic systems and are also connected to Kondo lattice systems.

## I. INTRODUCTION

Spin-boson models play a major role in various branches of physics, from condensed-matter physics, quantum optics, quantum dissipation, to quantum computation [1–4]. First, a large collection of harmonic oscillators (bosons) can simulate dissipation in quantum mechanics resulting in the celebrated Caldeira-Leggett model [5]. Through a two-level system coupled to a bath of bosons, one can also address the concept of dissipation-induced quantum phase transitions observed in various contexts [6, 7]. For example, a ohmic bosonic bath can be engineered through a long transmission line or a one-dimensional Luttinger liquid [8, 9]. An environment can also affect the critical exponents associated with a phase transition such as the disordered-ordered transition in the quantum Ising chain [10–15].

In this article, we develop a stochastic scheme in real time to address quantitatively the dynamics of quantum spin chains in the presence of a (ohmic) bosonic bath (and not only the steady state limit). This rather light formalism has been previously introduced for one spin-1/2 dissipative particle [16–21], random surfaces [22], dissipative light-matter systems [23] and Brownian motion [24]. This allows to address many-body quantum physics and strongly-dissipative non-equilibrium protocols [2, 3]. A distinct stochastic wave function approach formalism was also implemented [25, 26]. We consider a problem of two spins-1/2 in a ohmic bosonic bath and the dissipative Ising chain in a transverse field with long-range forces. We extend the formalism for two spins in an exact manner, and we introduce a dynamical mean-field treatment for the spin array allowing to describe non-equilibrium protocols such as Landau-Zener transitions and Kibble-Zurek mechanisms. We shall assume long-range forces between spins for the array, then resulting in a stochastic non-equilibrium mean-field theory. We present several applications of the formalism beyond the state of the art. We note that recent theoretical works have also addressed similar questions regarding the ef-

fects of macroscopic dissipation on the dynamical properties of quantum spin arrays [27–29]. Other methods have been devised to study the real-time spin dynamics in these spin-boson systems, such as Time Dependent Numerical Renormalization Group approaches [30–32], with recent progress done concerning the treatment of driving and quenches [33], and Matrix Product States [27, 34, 35]. Stochastic mean-field methods also allow to describe non-equilibrium light-matter systems [23, 36]. It is also relevant to mention that similar stochastic methods have been discussed previously for problems at equilibrium, in relation with disordered systems and quantum spin models [37–39].

### A. Model

Hereafter, we focus on a quantum Ising chain of  $M$  interacting spins, which are coherently coupled to one common bath of harmonic oscillators:

$$H = \frac{\Delta}{2} \sum_{p=1}^M \sigma_p^x + \sum_{p=1}^M \sum_k \lambda_k e^{ikx_p} \left( b_{-k}^\dagger + b_k \right) \frac{\sigma_p^z}{2} - \frac{K}{M} \sum_{p \neq r} \sigma_p^z \sigma_r^z + \sum_k \omega_k b_k^\dagger b_k. \quad (1)$$

Here,  $\sigma_p^\nu$  with  $\nu = \{x, y, z\}$  are Pauli matrices related to the spatial site  $p$  and the Planck constant  $\hbar$  is set to unity. At each site, the states  $|\pm_{z,p}\rangle$ , corresponding to the two eigenstates of  $\sigma^z$  with eigenvalues  $\pm 1$ , define the two possible orientations of the spin. The long-range ferromagnetic Ising interaction can be engineered in systems of trapped ions [40, 41] and ultra-cold atoms [42–45]. It can also be the result of the Van der Waals interaction in Rydberg media [46–48]. Exotic and non-equilibrium protocols, for example, based on many-body Rabi dynamics [49] or Ramsey interferences allow to investigate the properties of correlation functions in such systems [50],

or to devise a quantum thermometer [51]. Some theoretical studies have focused on the quenched dynamics across critical points, in spins [52–54] or bosonic systems [55–57]. Dynamics in quantum Ising chains has also been analyzed based on a Majorana fermion approach in the absence of the dissipative bath [58–60].

### B. Bath effects

The interaction with the bath plays an important role and affects both the equilibrium and the dynamical properties of the system. This also results in the general concept of quantum bath engineering [43, 61–64]. The spin-bath interaction is fully characterized by the spectral function  $J(\omega) = \pi \sum_k \lambda_k^2 \delta(\omega - \omega_k)$ , where we assume  $\omega_k = v_s |k|$ . Hereafter, we shall focus on the case of ohmic dissipation, where the spectral function reads  $J(\omega) = 2\pi\alpha\omega \exp\left(-\frac{\omega}{\omega_c}\right)$  in the quantum (zero-temperature) limit. Here,  $\omega_c$  is a high energy cutoff and the dimensionless parameter  $\alpha$  quantifies the strength of the interaction with the bath. The latter also induces a strong Ising-type *ferromagnetic* interaction  $K'_{|j-p|}$  between the spins  $j$  and  $p$  [43], which is mediated by an exchange of bosonic excitations at low wave vectors. This interaction is reminiscent of the Ruderman-Kittel-Kasuya-Yosida interaction for Kondo lattices. The bosonic induced-coupling has been observed in light-matter systems [65–67], for example. This interaction can be exemplified by applying an exact unitary transformation  $\tilde{H} = V^{-1}HV$  on the Hamiltonian (1), with  $V = \exp\left\{\frac{1}{2} \sum_k \sum_{j=1}^M \sigma_j^z e^{ikx_j} \frac{\lambda_k}{\omega_k} (b_k - b_{-k}^\dagger)\right\}$ . The transformed Hamiltonian indeed reads:

$$\tilde{H} = \sum_{j=1}^M \frac{\Delta}{2} (\sigma_j^+ e^{i\Omega_j} + \sigma_j^- e^{-i\Omega_j}) - \sum_{j \neq r} K'_{|j-p|} \sigma_j^z \sigma_r^z + \sum_k \omega_k b_k^\dagger b_k, \quad (2)$$

where  $\Omega_j = i \sum_k \frac{\lambda_k}{\omega_k} e^{ikx_j} (b_k - b_{-k}^\dagger)$ . Note that  $K'_{|j-p|} = \frac{K}{M} + K'_{|j-p|}$  explicitly denotes the renormalized Ising coupling between the spins  $j$  and  $p$ ,

$$K'_{|j-p|} = \frac{\alpha\omega_c}{2} \frac{1}{1 + \frac{\omega_c^2 (x_j - x_p)^2}{v_s^2}}. \quad (3)$$

The excitation of the spin  $j$  comes with a simultaneous polarization of the neighboring bath into a coherent state  $|\Omega_j\rangle = e^{i\Omega_j}|0\rangle$ , and the effective field seen by the spin is dressed by the presence of the bosonic modes. It results in a renormalization of the tunneling element  $\Delta$  to  $\Delta_r = \Delta(\Delta/\omega_c)^{\frac{\alpha}{1-\alpha}}$  [2, 3].

Below, we investigate the nonequilibrium dynamical properties of this system in the thermodynamic limit ( $M \rightarrow \infty$ ), and also for two spins ( $M = 2$ ). The two-spin

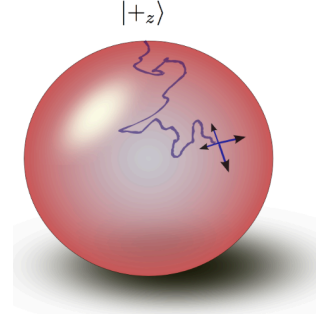


FIG. 1. (color online) Example of stochastic trajectories on the Poincaré or Bloch sphere. At each time  $t$ , we average the Schrödinger equation over Hubbard-Stratonovich variables which capture the informations of the bath degrees of freedom. A path is encoded into the Blip and Sojourn variables [2, 3] then providing an alternative description to the Keldysh contour. In this paper, we restrict ourselves to the zero-temperature limit for the environment, where quantum effects are important. The non-Markovianity of the dissipative environment at low temperatures is then hidden in the functions  $Q_1(t)$  and  $Q_2(t)$  in Eq. (16).

situation with the Hamiltonian in Eq. (1) is known to reveal a Kosterlitz-Thouless type quantum phase transition [30, 68, 69].

The rest of the paper is organized as follows. In Sec. II, we flesh out certain aspects of the methodology to compute the spin dynamics in the context of the spin array and for two spins. In Sec. III, we investigate the quantum phase transitions displayed by these systems, and present several results concerning the dynamics in the ordered phase in the case of two dissipative spins [30]. In the case of two spins, the universality class of the quantum phase transition induced by the (macroscopic) bath is of Kosterlitz-Thouless type [30]. For the spin array, the quantum phase transition is a second-ordered phase transition; the bath however can affect the critical exponents (in particular, the dynamical critical exponent  $z$ ) [14, 15, 30]. Then, we shall present in Sec. IV distinct protocols of Landau-Zener-Stueckelberg-Majorana interferometry [70–73] in the presence of tunable dissipation. In the case of two spins, the interaction mediated by the bath permits a great control over the system, allowing us to propose an entanglement protocol between the two spins thanks to bath engineering. In the case of the spin array, we apply a Kibble-Zurek type argument to account for the mean-field dynamics.

## II. METHOD

We tackle the real-time spin dynamics by using a stochastic approach which relies on the Feynman-Vernon path integral approach in real time [76] and the “Blip-Sojourn” (quantum jump) approach [2, 3]. A stochastic unravelling of the influence functional allows us to write the dynamics of the spin-reduced density matrix as a so-

lution of a stochastic differential equation [16–20, 23]. The Blip-Sojourn approach leads to an alternative implementation of the Keldysh contour [77, 78]. We extend previous works in an exact manner for the case of two spins, and at a mean field level for the spin array in the thermodynamical limit  $M \rightarrow \infty$ . A cartoon illustrating the method is shown in Fig. 1.

At a given time  $t$ , the elements of the spin reduced density matrix can be expressed as

$$\langle \sigma_f | \rho_S(t) | \sigma'_f \rangle = \sum_n \langle u_n, \sigma_f | U(t) \rho(t_0) U^\dagger(t) | u_n, \sigma'_f \rangle, \quad (4)$$

where we define  $|\sigma\rangle = |\sigma_1, \sigma_2, \dots, \sigma_M\rangle$ .  $\{u_n\}$  is a basis of the bosonic space and  $U$  the time-evolution operator of the whole system. For all sites we assume that spin and bath are uncoupled at the initial time  $t_0$  when they are brought into contact, so that the total density matrix

can be factorized. In the following, the initial state of the bath will always be a thermal state at inverse temperature  $\beta$ . All the spins are initially in the state  $|+_z\rangle$  so that  $\rho_S(t_0) = \prod_{j=1}^M |+_z, j\rangle \langle+_z, j| \equiv |+\rangle \langle+|$ .

The time-evolution of the spin reduced density matrix can be re-expressed thanks to a path integral description,

$$\langle \sigma_f | \rho_S(t) | \sigma'_f \rangle = \int D\sigma D\sigma' \exp \{i[S_\sigma - S_{\sigma'}]\} \mathcal{F}_{[\sigma, \sigma']}. \quad (5)$$

The integration runs over all  $M$ -dimensional paths  $\sigma$  and  $\sigma'$  such that  $|\sigma(t_0)\rangle = |\sigma'(t_0)\rangle = |+\rangle$ ,  $|\sigma(t)\rangle = |\sigma_f\rangle$  and  $|\sigma'(t)\rangle = |\sigma'_f\rangle$ .  $S_\sigma$  denotes the free amplitude to follow one given  $M$ -dimensional spin path without the environment, whose effect is contained in the influence functional  $\mathcal{F}_{[\sigma, \sigma']}$  [76]. Using the properties of gaussian integration, the influence functional can be expressed in a more convenient manner [2, 3]:

$$\mathcal{F}[\sigma, \sigma'] = e^{-\frac{1}{\pi} \int_{t_0}^t ds \int_{t_0}^s ds' \sum_{i,j} \left\{ -i\mathcal{L}_1(s-s', x_i-x_j) \frac{\sigma_i(s)-\sigma'_i(s)}{2} \frac{\sigma_j(s')+\sigma'_j(s')}{2} + \mathcal{L}_2(s-s', x_i-x_j) \frac{\sigma_i(s)-\sigma'_i(s)}{2} \frac{\sigma_j(s')-\sigma'_j(s')}{2} \right\}} \times \mathcal{G}[\sigma, \sigma'], \quad (6)$$

where  $\mathcal{L}_1$  and  $\mathcal{L}_2$  read:

$$\begin{aligned} \mathcal{L}_1(t, x) &= \frac{1}{2} \left[ L_1 \left( t - \frac{x}{v_s} \right) + L_1 \left( t + \frac{x}{v_s} \right) \right] \\ \mathcal{L}_2(t, x) &= \frac{1}{2} \left[ L_2 \left( t - \frac{x}{v_s} \right) + L_2 \left( t + \frac{x}{v_s} \right) \right]. \end{aligned} \quad (7)$$

Similar to the one-spin situation, we have in the quantum limit where  $\beta \rightarrow +\infty$ ,

$$\begin{aligned} L_1(t) &= \int_0^\infty d\omega J(\omega) \sin \omega t, \\ L_2(t) &= \int_0^\infty d\omega J(\omega) \cos \omega t. \end{aligned} \quad (8)$$

For an ohmic bath, the functions  $L_1$  and  $L_2$  explicitly read,

$$\begin{aligned} L_1(t) &= 4\pi\alpha\omega_c^2 \frac{\omega_c t}{(1 + \omega_c^2 t^2)^2} \\ L_2(t) &= 2\pi\alpha\omega_c^2 \frac{1 - \omega_c^2 t^2}{(1 + \omega_c^2 t^2)^2}. \end{aligned} \quad (9)$$

From Eq. (7), we see that the bosonic environment couples the symmetric and anti-symmetric classical spin paths  $\eta_p(t) = 1/2[\sigma_p(t) + \sigma'_p(t)]$  and  $\xi_p(t) = 1/2[\sigma_p(t) - \sigma'_p(t)]$  at different times and different lattice sites. These spin variables take values in  $\{-1, 0, +1\}$  and are the equivalent of the classical and quantum variables in the Schwinger-Keldysh representation. In Fig. 2, we plot the space and time coupling functions  $\mathcal{L}_1$  (bottom left) and  $\mathcal{L}_2$  (bottom right). We

see that the bosons induce a long-range interaction between spins. The maximal effect between two spins separated by a distance  $x$  occurs after a time  $x/v_s$ , due to the finite sound velocity  $v_s$  of the excitations.

The last term of Eq. (6) reads

$$\mathcal{G}[\sigma, \sigma'] = e^{i\frac{\mu}{2} \int_{t_0}^t ds \left[ \sum_j \frac{\sigma_j(s)}{2} e^{ikx_j} \right]^2 - \left[ \sum_j \frac{\sigma'_j(s)}{2} e^{ikx_j} \right]^2}, \quad (10)$$

with  $\mu = 2/\pi \int_0^\infty J(\omega)/\omega$ . We recover that the bath is responsible from an indirect *ferromagnetic* Ising-like interaction between the spins  $K'_{|j-p|} = 1/(2\pi) \int_0^\infty J(\omega)/\omega \cos[(x_i - x_j)/v_s]$  (see Eq. (3)).

We have shown that the bath is responsible for two distinct types of interactions. The first one is a retarded interaction mediated by the bosonic excitations, which travel at the speed  $v_s$ . The second one is an instantaneous interaction  $K'$ , of which we have given a physical interpretation thanks to the polaronic transformation in Eq. (2). Dealing with the spatial extent remains difficult, and we will treat the array problem at a mean-field model, while the two-spin model is tractable in an exact manner.

## A. Array

We treat direct spin-spin Ising interactions, which are contained in  $S_S$  and  $S_{S'}$ , by introducing two auxiliary

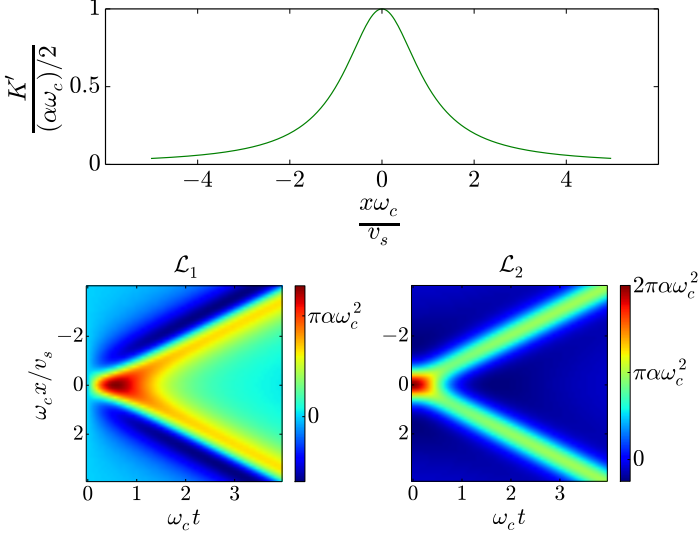


FIG. 2. (color online) Top: Evolution of the direct Ising interaction which is induced by the presence of the bath between two spins distant of  $x$ , as a function of  $x\omega_c/v_s$ . Bottom: Space-time dependency of the coupling functions  $\mathcal{L}_1$  (left) and  $\mathcal{L}_2$  (right). The bath induces a long-range interaction between spins.

fields  $\chi_1$  and  $\chi_2$ , such that:

$$S_{Ising} = \int D\chi_1 \exp \left[ \int_{t_0}^t ds \frac{M\chi_1^2(s)}{2iK} + \chi_1(s) \sum_{p=1}^M \sigma_p(s) \right] \times \int D\chi_2 \exp \left[ - \int_{t_0}^t ds \frac{M\chi_2^2(s)}{2iK} + \chi_2(s) \sum_{p=1}^M \sigma'_p(s) \right] \quad (11)$$

We then use a stationary phase approximation on the fields  $\chi_1$  and  $\chi_2$  in order to estimate the mean-field effect of the Ising coupling:  $\chi_1(s) = -\frac{iK}{M} \sum_{p=1}^M \sigma_p(s)$  and  $\chi_2(s) = \frac{iK}{M} \sum_{p=1}^M \sigma'_p(s)$ . In the thermodynamic limit  $M \rightarrow \infty$ , we introduce  $S^z(s) = \frac{1}{M} \sum_{p=1}^M \sigma_p(s)$  such that  $\langle S^z(s) \rangle = \langle \sigma^z(s) \rangle$ . The coupling between spins in Eq. (11) is then replaced by a local interaction. This mean-field approximation is valid in the thermodynamic limit  $M \rightarrow \infty$ . Finally the propagation integral can be factorized in a product of  $M$  individual matrix elements, so that it is possible to write (we drop the  $p$  index in the following, as all the sites are equivalent):

$$\langle \sigma_{p,f} | \rho_{S,p}(t) | \sigma'_{p,f} \rangle = \int D\sigma D\sigma' A_p[\sigma_p] A_p[\sigma'_p]^* F[\sigma_p, \sigma'_p] \times e^{-iK_r \int_{t_0}^t ds [\sigma_p(s) - \sigma'_p(s)] \langle \sigma^z(s) \rangle} \quad (12)$$

where  $\rho_{S,p}$  denotes the density matrix of spin  $p$ .

The next step is to rewrite the spin path in the language of “Blips” and “Sojourns”, following the seminal

work of Ref. [2]. This step was carefully described in the case of one single spin in Refs. [2, 3, 16, 17, 23], and will not be explicited here. We will however fully describe the derivation in the case of two spins in the next subsection. After the introduction of a “Blips” and “Sojourns” variables and a stochastic unraveling of the influence functional [16, 18, 23], it is possible to write:

$$\frac{1 + \langle \sigma^z(t) \rangle}{2} = \overline{\langle \Phi_f | T e^{-i \int_{t_0}^t ds \frac{\Delta}{2} V(s)} | \Phi_i \rangle}, \quad (13)$$

where  $T$  is the time-ordering operator and the effective stochastic Hamiltonian for the spin density matrix is

$$V = \begin{pmatrix} 0 & e^{-h-h_I+k} & -e^{h+h_I+k} & 0 \\ e^{h+h_I-k} & 0 & 0 & -e^{h+h_I+k} \\ -e^{-h-h_I-k} & 0 & 0 & e^{-h-h_I+k} \\ 0 & -e^{-h-h_I-k} & e^{h+h_I-k} & 0 \end{pmatrix}. \quad (14)$$

The overline denotes a statistical average, and  $h$  and  $k$  are two complex gaussian random fields, which verify:

$$\begin{aligned} \overline{h(t)h(s)} &= \frac{1}{\pi} Q_2(t-s) + l_1 \\ \overline{k(t)k(s)} &= l_2 \\ \overline{h(t)k(s)} &= \frac{i}{\pi} Q_1(t-s)\theta(t-s) + l_3, \end{aligned} \quad (15)$$

where  $l_i$  are arbitrary complex numbers which do not contribute. This formalism gives rise to a stochastic jump description on the Bloch sphere. All the effects of quantum memory is now captured in these additional time-correlated stochastic degrees of freedom. The two coupling functions  $Q_1$  and  $Q_2$  are the second integrals of the  $L_1$  and  $L_2$  functions and they read at zero temperature:

$$\begin{aligned} Q_1(t) &= 2\pi\alpha \tan^{-1}(\omega_c t) \\ Q_2(t) &= \pi\alpha \log(1 + \omega_c^2 t^2). \end{aligned} \quad (16)$$

These functions are related to the time correlations of the operators  $\hat{h}_j = e^{i\Omega_j}$  introduced in Eq. (2);  $\langle \hat{h}_j(t) \hat{h}_j^\dagger(s) \rangle = \exp \{ 1/\pi [iQ_1(t-s) - Q_2(t-s)] \}$ . The effect of the interaction between the spins can be seen through the field  $h_I$ , which explicitly depends on  $\langle \sigma^z(t) \rangle$ ,  $h_I(t) = -2iK \int_{t_0}^t ds \langle \sigma^z(s) \rangle$ .

By analogy with the single spin-1/2 problem [23], the vector  $|\Phi(t)\rangle$  represents the double spin state which characterizes the spin density matrix. As can be seen from Eq. (14) the tunneling element  $\Delta$  is now dressed by the environment and picks up a phase characterized by the two stochastic fields  $h$  and  $k$ , reminiscent of the form of the polaron-transformed Hamiltonian (see Eq. (2)). We have  $|\Phi_i\rangle = (e^{k(t_0)}, 0, 0, 0)^T$  and  $\langle \Phi_f | = (e^{-k(t_{2n})}, 0, 0, 0)$ : these choices account for the asymmetry between blips and sojourns. The contribution from the first sojourn is encoded in  $|\Phi_i\rangle$ , and we artificially suppress the contribution of the last sojourn via  $|\Phi_f\rangle$ . This final vector

depends on an intermediate time, but we can notice that replacing  $(e^{-k(t_{2n})}, 0, 0, 0)$  by  $(e^{-k(t)}, 0, 0, 0)$  does not add any contribution on average.

In the scaling regime  $\Delta/\omega_c \ll 1$ , the  $Q_1$  function in Eq. (16) can be considered as a constant ( $\tan^{-1}(\omega_c t) \simeq \pi/2$ ). This allows us to use only one stochastic field, improving the numerical convergence efficiently [16].

## B. Two spins: Exact method

In the case of two spins, it is possible to reach an exact linear and local stochastic differential equation describing the dynamics of the spin reduced density matrix. Eqs. (6) and (10) are still valid for  $M = 2$ . In particular, we find that the Ising interaction is explicitly renormalized as  $K_r = K + \alpha\omega_c$  as we have,

$$\mathcal{G}[\sigma_1, \sigma_2, \sigma'_1, \sigma'_2] = \exp \left\{ \int_{t_0}^t ds K_r [\sigma_1(s)\sigma_2(s) - \sigma'_1(s)\sigma'_2(s)] \right\}. \quad (17)$$

The derivation of the next steps of the method relies on the generalization of the “Blip” and “Sojourn” development introduced in Ref. [2] in the case of two spins. It basically consists to rewrite the spin integration in an explicit manner, by considering all the possible spin paths.

### 1. Blip and Sojourn development

In the case of the two spin system, the series development can be viewed as a single path that visits sixteen states corresponding to the matrix elements of the spin-reduced density-matrix. Let us suppose that the spin subsystem starts in the state  $|+_{z,1}, +_{z,2}\rangle$ , and that we intend to compute the probability  $p(t) = \langle +_{z,1}, +_{z,2} | \rho_S(t) | +_{z,1}, +_{z,2} \rangle$  to come back in the state  $|+_{z,1}, +_{z,2}\rangle$  at time  $t$ . Then, both the first and the second spin path make an even number of transitions along the way at times  $t_j^p$ ,  $j \in \{1, 2, \dots, 2n_p\}$  for  $p \in \{1, 2\}$  such that  $t_0^p < t_1^p < t_2^p < \dots < t_{2n_p}^p$ . We can write these spin paths as  $\xi_p(t) = \sum_{j=1}^{2n_p} \Xi_j^p \theta(t - t_j^p)$  and  $\eta_p(t) = \sum_{j=0}^{2n_p} \Upsilon_j^p \theta(t - t_j^p)$  where the variables  $\Xi_j^p$  and  $\Upsilon_j^p$  take values in  $\{-1, 1\}$ .

The diagonal element of the density matrix describing the probability to come back in the state  $|+_{z,1}, +_{z,2}\rangle$  at time  $t$  is given by a series in the tunneling coupling  $\Delta^2$ :

$$p(t) = \sum_{N=0}^{\infty} \left( \frac{i\Delta}{2} \right)^{2N} \int_{s_0}^t ds_{2N} \dots \int_{s_0}^{s_2} ds_1 \sum_{\{\Xi_j^p\}, \{\Upsilon_j^p\}} \mathcal{F}_{n_1, n_2}. \quad (18)$$

where  $N = n_1 + n_2$  and  $\{s_0, s_1, \dots, s_{2(n_1+n_2)}\}$  is the ordered reunion of the two sequences  $\{t_j^1\}$  and  $\{t_j^2\}$ . The

prime in  $\{\Upsilon_j^p\}'$  in Eq. (18) indicates that the initial and final states are fixed according to  $\Upsilon_0^1 = \Upsilon_0^2 = \Upsilon_{2n_1}^1 = \Upsilon_{2n_2}^2 = 1$ . The influence functional can be written explicitly in terms of these “blips” and “sojourn” variables:

$$\mathcal{F}_{n_1, n_2} = \prod_{p=1}^2 \mathcal{Q}_1^p \mathcal{Q}_2^p \mathcal{M}_1^p \mathcal{M}_2^p \quad (19)$$

$$\mathcal{Q}_1^p = \exp \left[ \frac{i}{\pi} \sum_{k=0}^{2n_p-1} \sum_{j=k+1}^{2n_p} \Xi_j^p \Upsilon_k^p Q_1(t_j^p - t_k^p) \right] \quad (20)$$

$$\mathcal{Q}_2^p = \exp \left[ \frac{1}{\pi} \sum_{k=1}^{2n_p-1} \sum_{j=k+1}^{2n_p} \Xi_j^p \Xi_k^p Q_2(t_j^p - t_k^p) \right] \quad (21)$$

$$\mathcal{M}_1^p = \exp \left[ \frac{i}{\pi} \sum_{k=0}^{2n_q-1} \sum_{j:t_j^p > t_k^q} \Xi_j^p \Upsilon_k^q Q_1(t_j^p - t_k^q) \right] \quad (22)$$

$$\mathcal{M}_2^p = \exp \left[ \frac{1}{\pi} \sum_{k=1}^{2n_q-1} \sum_{j:t_j^p > t_k^q} \Xi_j^p \Xi_k^q Q_2(t_j^p - t_k^q) \right]. \quad (23)$$

The Ising interaction can be expressed in a convenient way in the “blip” and “sojourn” description, as we have

$$\sigma_1(s)\sigma_2(s) - \sigma'_1(s)\sigma'_2(s) = 2[\eta_1(s)\xi_2(s) + \eta_2(s)\xi_1(s)]. \quad (24)$$

### 2. Stochastic decoupling

After a stochastic unravelling of the influence functional, it is possible to reach a Stochastic Schrödinger Equation, where the effective time-dependent Hamiltonian reads

$$V(t) = \frac{\Delta}{2} \begin{pmatrix} W_2 & D_{B \rightarrow A} & D_{C \rightarrow A} & (0) \\ D_{A \rightarrow B} & W_2 & (0) & D_{D \rightarrow B} \\ D_{A \rightarrow C} & (0) & W_2 & D_{D \rightarrow C} \\ (0) & D_{B \rightarrow D} & D_{C \rightarrow D} & W_2 \end{pmatrix}. \quad (25)$$

The matrix  $W_2$  has the same structure as in the one-spin case,

$$W_2(t) = \begin{pmatrix} 0 & e^{-h+k} & -e^{h+k} & 0 \\ e^{h-k} & 0 & 0 & -e^{h+k} \\ -e^{-h-k} & 0 & 0 & e^{-h+k} \\ 0 & -e^{-h-k} & e^{h-k} & 0 \end{pmatrix}. \quad (26)$$

The eight matrices  $D_{B \rightarrow A}$ ,  $D_{C \rightarrow A}$ ,  $D_{A \rightarrow B}$ ,  $D_{D \rightarrow B}$ ,  $D_{A \rightarrow C}$ ,  $D_{D \rightarrow C}$ ,  $D_{B \rightarrow D}$  and  $D_{C \rightarrow D}$  are four by four diagonal matrices which are respectively  $e^{-h+k} \times I_4$ ,  $-e^{h+k} \times I_4$ ,  $e^{h-k} \times I_4$ ,  $-e^{h+k} \times I_4$ ,  $-e^{-h-k} \times I_4$ ,  $e^{-h+k} \times I_4$ ,  $-e^{-h-k} \times I_4$  and  $-e^{-h-k} \times I_4$  ( $I_4$  is the identity). The fields  $h$  and  $k$  verify the correlations

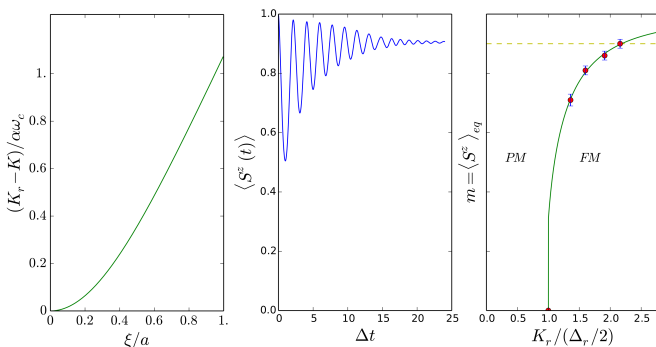


FIG. 3. (color online) Left: Evolution of the part of the Ising interaction which is induced by the presence of the bath, as a function of  $\xi/a$  where  $\xi = v_s/\omega_c$  and  $a$  the lattice spacing. The cutoff frequency is fixed to  $\omega_c = 100\Delta$ . Center: Dissipative dynamics of the spin  $\langle S^z(t) \rangle$  in the ferromagnetic phase, for  $\alpha = 5.0 \cdot 10^{-2}$ . Right: Magnetization per site  $m$  with respect to the Ising coupling. The full green line corresponds to the theoretical evolution of  $m$ . FM and PM refer to the Ferromagnetic and Paramagnetic phases.

of Eq. (15).  $|\Phi_i\rangle$  and  $|\Phi_f\rangle$  are determined in accordance with the initial final conditions. Here, we have  $|\Phi_i\rangle = (e^{-2k(t_0)}, 0, 0, 0, 0, 0, 0, 0, 0, 0, 0, 0, 0, 0, 0, 0)$ . Other initial or final conditions lead to a different choice for these vectors.

Similarly to the one-spin case, simplifications occur in the scaling regime. This procedure can be equivalently developed in the triplet/singlet basis, where we define triplet subspace is spanned by the three states  $\{|T_-\rangle = |-z -z\rangle, |T_0\rangle = 1/\sqrt{2} [|+z -z\rangle + |-z +z\rangle], |T_+\rangle = |+z +z\rangle\}$ , and the singlet state is  $|S\rangle = 1/\sqrt{2} [|+z -z\rangle - |-z +z\rangle]$ .

### III. FREE DYNAMICS AND QUANTUM PHASE TRANSITION

In this part we apply the methodology developed in the previous section to tackle the nonequilibrium spin dynamics in the presence of strong dissipative interactions. First we investigate the effect of the bath on the mean-field Ising transition, and find that its presence renormalizes the critical coupling. This point has been previously noticed in Ref. [43]. We then present results concerning the quench dynamics of two spins in the ordered phase (or localized phase induced by dissipation).

#### A. Array

The Ising interaction is renormalized to  $K_r = K + 2\sum_{j=1}^{\infty} K'_j$  (see Fig. 3). As a test of the method, we check that the steady states of the dynamics lead to correct thermodynamical properties in the dissipative quantum Ising chain with long-range forces, as can be seen in

the right panel of Fig. 3, with a renormalization of the critical coupling to  $K_c \simeq \Delta_r/2$ . The bath causes then a decay towards one of the two equilibrium states in the ferromagnetic phase as well as a renormalization of both the tunneling element and the Ising coupling. However, it does not affect the dynamical properties of the quantum phase transition as long as the direct Ising term  $K$  is *not* zero. This behavior can be understood thanks to a thermodynamic analysis of the action at low wave-vectors  $q$  and low frequency  $\omega$ , which is dominated by the peaked contribution at  $q = 0$  of the long range Ising interaction, as shown in Appendix A. We also develop a toy model for the spin dynamics with the equations of motions, which is valid at weak coupling, and we find back the correct equilibrium features (see Appendix B).

Below, we address various nonequilibrium protocols which have not been addressed in the literature to our knowledge, such as the quench dynamics of the dimer model in the localized phase, and dissipative Landau-Zener protocols for both the dimer and the array.

#### B. Two spins

The two-spin problem is well-known to exhibit a dissipative quantum phase transition [30, 68, 69] where the bath entirely polarizes the two spins either in the  $|T_+\rangle$  or  $|T_-\rangle$  state, by analogy to a ferromagnetic phase [30]. We reproduce this transition within our method (we will discuss more thoroughly this point in Sec. IV B). We are also able to address the non-equilibrium dynamics of the system in the localized and strongly dissipative phase, starting from the nonequilibrium state  $|T_0\rangle$ . In particular, we confirm an exponential relaxation towards the equilibrium states  $|T_+\rangle$  and  $|T_-\rangle$ ,  $p_{|T_0\rangle}(t) = \exp(-\Gamma t)$ . The relaxation rate obeys  $\Gamma \propto (\nu - \alpha)(\Delta/\omega_c)^2$ , where  $\nu$  is a constant with respect to  $\Delta$  and  $\alpha$  (see Fig. 4).

### IV. LANDAU-ZENER TRANSITIONS

In this section, we go further and investigate the non-equilibrium behavior of this system under an additional linear driving term  $\epsilon(t)/2\sum_j \sigma_j^z$  with  $\epsilon(t) = \epsilon_0 + vt$ , ( $v > 0$ ). We choose  $\epsilon_0 < 0$  so that the initial state  $|+\rangle = \prod_p |+_p, z\rangle$  corresponds to the ground state at the initial time  $t = 0$ . Driving terms can be easily accounted for in the stochastic method [16, 23]. Landau [70], Zener [71], Stueckelberg [72] and Majorana [73] provided an analytical description of this problem in the case of an isolated two-level system subject to a linear sweep ( $K = 0$  and  $\alpha = 0$ ). The survival probability  $p_{lz}$  that the spin remains in its initial state after the sweep, is fully determined by the velocity of the sweep  $v$ , and we have  $p_{lz} = \exp[-\pi\Delta^2/2v]$ . It was shown in Refs. [17, 74, 75] that the presence of a gaussian dissipative bath does not affect the transition probability in the case of the Landau-Zener sweep for one single spin, as long as the coupling



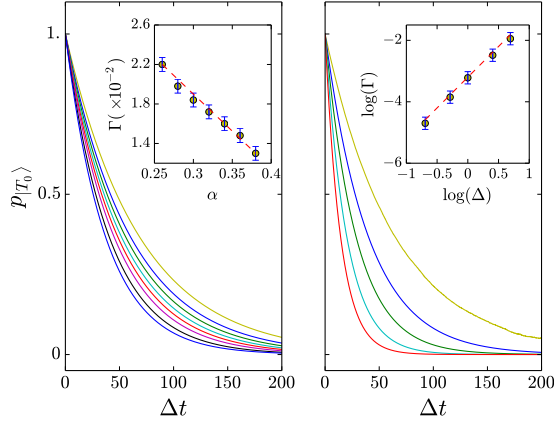


FIG. 4. Quench dynamics of the dimer model in the localized phase. The system starts in the state  $|T_0\rangle$  in both plots, and relax towards a statistic superposition of  $|T_+\rangle$  and  $|T_-\rangle$ . Left panel: the different curves correspond to different values of  $\alpha$  ranging from 0.24 to 0.38. Inset: evolution of the relaxation rate  $\Gamma$  as a function of  $\alpha$ . Right panel: the different curves correspond to different values of  $\Delta$  ranging from 0.5 to 2. Inset: evolution of the logarithm of the relaxation rate  $\Gamma$  as a function of the logarithm of the tunneling element  $\Delta$ .

is along the z-direction. It is no longer true when there are several spins and the presence of the bath affects the final state for both the array and the dimer case.

### A. Array

We focus on rather fast many-body Landau-Zener sweeps for the array, at a mean-field level. Let us underline that this protocol is different from the dynamical transition of the quantum Ising model in transverse field with nearest neighbours interactions studied in the literature [58, 59] (and references therein), where the driving parameter is the transverse field and which can be studied elegantly in  $k$  space. Here, we are interested in the dynamics of local spin variables at a mean field level. A rigorous description of the dynamics should involve all the energy levels of the system, and their respective anti-crossings. Our mean-field description greatly simplifies the problem and the interplay of all the levels is reduced to a single anti-crossing governed by the local self-consistent Hamiltonian,

$$H_j = \frac{\Delta}{2} \sigma_j^x + \left[ \frac{\epsilon(t)}{2} - K_r \langle \sigma^z(t) \rangle \right] \sigma_j^z + \sum_k \left[ \lambda_k e^{ikx_j} (b_{-k}^\dagger + b_k) \frac{\sigma_j^z}{2} + \omega_k b_k^\dagger b_k \right]. \quad (27)$$

The presence of the Ising interaction or the presence of the bath both lead to a change in the final value of  $\langle \sigma^z(t \rightarrow \infty) \rangle$ . The origin is the same in both cases. At weak coupling, the dominant effect of the bath is indeed

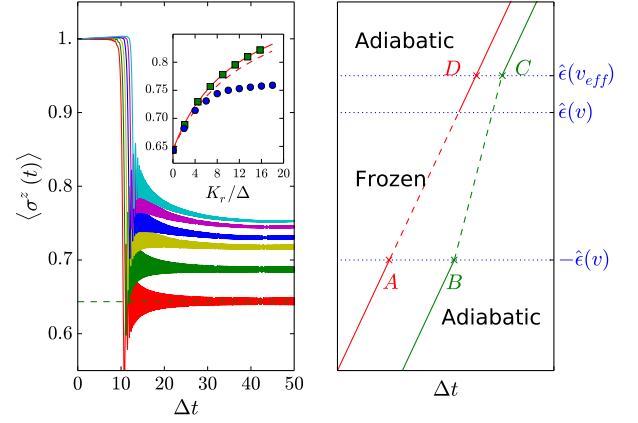


FIG. 5. Left: Fast sweep ( $v/\Delta^2 = 8$ ) in the array, for different values of  $\alpha$  corresponding to  $K_r$  from 0 to 10 ( $K = 0$  for the main figure,  $\omega_c = 100\Delta$ ). Inset: the full (dashed) red line shows the expectation value of  $\langle \sigma^z(t \rightarrow \infty) \rangle$  with respect to  $K_r/\Delta$  ( $K_r/\Delta_r$ ) deduced from the Kibble-Zurek mechanism. Green squares: results for a direct Ising interaction  $K_r = K$ . Blue points: results for an interaction mediated by the bath  $K = 0$ . Right: schematic interpretation of the Landau-Zener sweep for the array in the framework of the Kibble-Zurek mechanism. The line (AD) shows the evolution of the bare bias field with respect to time, while the broken line connecting points B and C represents the effective bias field. The lines are full during the adiabatic stages, and dashed during the frozen (non-adiabatic) period.

to induce a ferromagnetic Ising-like interaction  $K_r$ . In the following we use a Kibble-Zurek argument [79, 80] in order to describe quantitatively this effect. The single site fast Landau-Zener transition can indeed be described thanks to the Kibble-Zurek mechanism, which predicts the production of topological defects in nonequilibrium phase transitions [59, 79–82]. This description splits the dynamics into three consecutive stages: it is supposed to be adiabatic in the first place, then evolves in a non-adiabatic way near the transition point, and finally becomes adiabatic again. The impossibility of the order parameter to follow the change applied on the system provokes this non-adiabatic stage, where the dynamics is said to be “frozen”. It is convenient to introduce the characteristic energy scale [82]

$$\hat{\epsilon} = 1/\sqrt{2} \left\{ \left[ 1 + 16v^2/(\pi^2 \Delta^4) \right]^{1/2} - 1 \right\}^{1/2}, \quad (28)$$

which sets the limit between adiabatic and frozen stages (see Fig. 5).

When the Ising interaction is not zero, the effective field felt by one site is the sum of the bias field  $\epsilon(t)$  and the Ising interaction, and will be denoted  $\epsilon_{eff}(t)$ . The dynamics always enters in the frozen stage with  $\langle \sigma^z \rangle \simeq 1$ , so that we have  $\epsilon_{eff}(t) = \epsilon(t) - K$  during the first adiabatic stage. At the end of the frozen stage, the spin expectation value has changed, and the effective field becomes

$\epsilon_{eff}(t) = \epsilon(t) - K\langle\sigma^z(t)\rangle$ . This leads to a change of the effective speed at which the frozen zone is crossed through, and ultimately of the transition probability. This can be seen on the right pannel of Fig. 5, where we show the evolution of both the bare and the effective bias fields with respect to time. We can estimate the renormalization of the effective speed self-consistently thanks to basic geometrical considerations in the trapezoid ( $ABCD$ ) of the Fig. 5. The effective crossing speed is given by

$$v_{eff} = \frac{\hat{\epsilon}(v) + \hat{\epsilon}(v_{eff})}{t_C(v_{eff}) - t_B}. \quad (29)$$

The denominator can be simplified by writing that  $t_C(v_{eff}) - t_B = [t_C(v_{eff}) - t_D] + (t_D - t_A) - (t_B - t_A)$ . We know that  $(t_D - t_A) = [\hat{\epsilon}(v) + \hat{\epsilon}(v_{eff})]/v$ , and  $[t_C(v_{eff}) - t_D] - (t_B - t_A)$  can be expressed as  $-K[1 - \langle\sigma^z(t_C, v_{eff})\rangle]$ . Next we suppose that we can approximate  $\langle\sigma^z(t_C, v_{eff})\rangle$  by  $\langle\sigma^z(t \rightarrow \infty)\rangle$ . Altogether, we get

$$\frac{v_{eff}}{v} = \frac{\hat{\epsilon}(v) + \hat{\epsilon}(v_{eff})}{\hat{\epsilon}(v) + \hat{\epsilon}(v_{eff}) - 2K[1 - p_{lz}(v_{eff})]}. \quad (30)$$

It allows us to know the variation of the effective speed  $v_{eff}$  at which the transition is crossed with respect to the Ising interaction  $K$ . The spin expectation value  $\langle\sigma^z(t \rightarrow \infty)\rangle$  is then estimated thanks to the Landau-Zener formula, and its evolution with respect to  $K$  is shown by the red curve in the inset of the left part of Fig. 5. The dotted red curve takes into account the renormalization of the tunneling frequency  $\Delta_r$  due to the presence of the bath. The estimation matches well the results in the case of a direct Ising interaction at  $\alpha = 0$ . At weak coupling, the dominant effect of the bath is to induce a ferromagnetic Ising-like interaction  $K_r$ . The estimation of the final value of the spin variable thanks to Eq. (30) is correct at small  $\alpha$  if we replace  $K$  by  $K_r$ . However, it breaks down when the dissipation strength is increased because the assumption  $\langle\sigma^z(t_C, v_{eff})\rangle \simeq \langle\sigma^z(t \rightarrow \infty)\rangle$  used to derive  $v_{eff}$  is no longer correct. Relaxation processes occur after the crossing of the frozen zone which lower  $\langle\sigma^z(t \rightarrow \infty)\rangle$ .

## B. Two spins

Now we address “non-local” protocols for two spins, with only the triplet states being coupled to the bath (the singlet  $|S\rangle = 1/\sqrt{2}[|+z-z\rangle - |-z+z\rangle]$  is not coupled for a symmetric drive). The dynamics in the triplet subspace spanned by the three states  $\{|T_-\rangle = |-z-z\rangle, |T_0\rangle = 1/\sqrt{2}[|+z-z\rangle + |-z+z\rangle], |T_+\rangle = |+z+z\rangle\}$  is governed by the driving term  $\epsilon(t)$  and by the strength of the coupling to the environment. We consider the following setup: initially at the time  $t_0$  the two spins are constrained in the state  $|T_+\rangle = |+z+z\rangle$  and we apply a linear sweep  $\epsilon(t) = \epsilon_0 + vt$ . Here, three levels

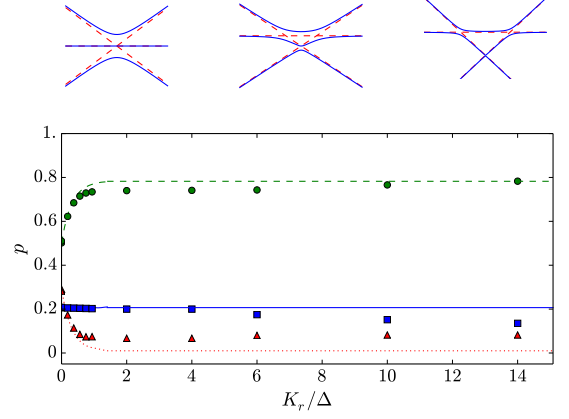


FIG. 6. Top: evolution of the energy levels with respect to the drive  $\epsilon$ , for different values of the direct Ising coupling at  $\alpha = 0$ . Main figure: evolution of the final transition probabilities after a linear sweep of velocity  $v = 2\Delta^2$  as a function of  $K_r/\Delta$ . The lines correspond to a direct Ising interaction  $K_r = K$ , and the markers correspond to a bath-induced coupling ( $K_r = \alpha\omega_c$ ). Full blue line, and blue squares:  $p_{|T_+\rangle}(t \rightarrow \infty)$ . Dotted red line and red triangles:  $p_{|T_-\rangle}(t \rightarrow \infty)$ . Dashed green line and green points:  $p_{|T_0\rangle}(t \rightarrow \infty)$ . We take  $\omega_c = 100\Delta$ .

participate to the dynamics and the system then constitutes a  $SU(3)$  Landau-Zener-Stueckelberg-Majorana interferometer [83].

In Fig. 6, we plot the different probabilities  $p_{|T\rangle}(t \rightarrow \infty)$ , for  $|T\rangle \in \{|T_-\rangle, |T_0\rangle, |T_+\rangle\}$  (dotted lines) to end up in the state  $|T\rangle$  at long times after a linear sweep of intermediate velocity  $v = 2\Delta^2$ , as a function of  $K/\Delta$  ( $\alpha = 0$ ). On the upper part, we draw the energy levels of the triplet states as a function of  $\epsilon$ , for different values of the Ising coupling. In all cases the system starts at time  $t = 0$  on the lower branch at negative bias  $\epsilon_0$ . At the velocity considered here, we go from the regime of independent crossings (the two spins behave independently when  $K = 0$ ) to the regime of one single crossing between  $|T_+\rangle$  and  $|T_0\rangle$  while we increase the value of  $K$ . When  $K/\Delta \gg 1$ , the lowest anticrossing can be ignored and the probability to end up in the state  $|T_-\rangle$  then vanishes as the first gap closes (see Fig. 6). The value of  $p_{|T_+\rangle}(t \rightarrow \infty)$  is not affected by the Ising interaction.

Similarly to the array case, the dominant effect of the bath is to induce a ferromagnetic Ising-like interaction, as can be seen in Fig. 6. Here, the probability to end up in the state  $|T_-\rangle$  does not vanish. This is due to transitions from  $|T_0\rangle$  to  $|T_-\rangle$  associated to emissions of a bosonic excitations after the crossing of the critical point. For very rapid transitions, losses become negligible and the fidelity is higher. Multiple consecutive and rapid passages may result in constructive or destructive interferences, depending on the phases acquired during the adiabatic



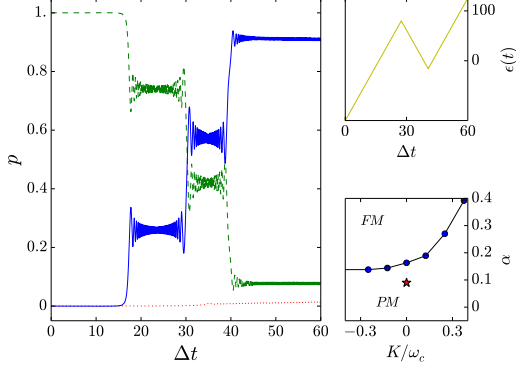


FIG. 7. Landau-Zener-Stueckelberg-Majorana interferometry in the strong-coupling (large  $K_r$ ) regime with two spins. We plot the occupation probabilities as a function of time. Dashed green line:  $p_{|T_+\rangle}(t)$ . Full blue line:  $p_{|T_0\rangle}(t)$ . Dotted red line:  $p_{|T_-\rangle}(t)$ . Here we have  $\alpha = 0.08$ ,  $\omega_c = 100\Delta$ . The insets show the time-dependent drive applied on the system as well as the phase diagram for the two-spin system.

and the non-adiabatic evolutions [84], allowing to propose an entanglement generation protocol by tuning the external drive, which is of great importance for quantum information purposes.

We use the bath to create fully entangled spin states, as can be seen in Fig. 7. The system starts from the state  $|T_+\rangle$  and ends in the entangled state  $|T_0\rangle$  at the end of the driving protocol, which corresponds to a non-equilibrium steady state of the problem. At intermediate times, the system is in “Schrödinger cat” states entangled with the environment, and we use this joint dynamics and the interaction mediated by the bath for entanglement purposes. A higher number of passages may result in a better fidelity thanks to a simple scaling argument. Losses due to relaxation processes typically

grow linearly with the time during which the levels are close in energy, so that the losses scale as  $1/v$  for one passage. Assuming additive interferences, the number of passages  $N$  needed to achieve a complete transition scales as  $\sqrt{v}$  at large velocity (see the oscillation frequency of the occupancies in the fast velocity case in Ref. [84]). The losses of the entire entanglement process scale then as  $1/\sqrt{v}$ , and the fidelity is higher for multiple passages at high speed.

## V. CONCLUSION

To summarize succinctly, we have developed a many-body stochastic approach to address quantum jumps in dissipative spin arrays. We have considered non-equilibrium protocols and quantum interferometry with bath engineering, both in the case of two spins and for the quantum Ising chain with long-range forces. We have presented results that go beyond the state of the art; for example, we have studied the dynamics of the dissipative dimer model in the localized (ferromagnetically ordered) phase as well as dissipative Landau-Zener protocols both for the dimer model and the spin array subject to long-range forces. For the latter situation, we have developed a single-crossing Kibble-Zurek type argument. These results can be tested in ultra-cold atom systems [42, 43, 51].

The method could also be applied to the sub-ohmic spin-boson model [85, 86], Jaynes-Cummings or Rabi arrays [23, 87], for topological problems with Dirac points [88], and for fermionic environments [77, 78, 89], as in Kondo lattices.

We thank Camille Aron, Erik Eriksson, Loïc Herviou, Walter Hofstetter, Christophe Mora, Peter P. Orth, Zoran Ristivojevic, Guillaume Roux, Marco Schiro for discussions. This work has been supported by PALM Labex, project Quantum-Dyna (ANR-10-LABX-003).

## Appendix A: Thermodynamic analysis of the action for the dissipative Ising model in transverse field

As shown in Fig. 1 in the main text, the mean-field dynamics is not affected by the presence of the bath. This behavior can be understood thanks to a thermodynamic analysis of the action at low wave-vectors  $q$  and low frequency  $\omega$ , which is dominated by the peaked contribution at  $q = 0$  of the long range Ising interaction. Using a mapping to a classical Ising model, it is possible to estimate the spin-spin coupling due to the environment:

$$\int D(b, b^*) e^{-S} = \exp \left\{ \frac{1}{4\pi} \int_0^\beta d\tau \int_0^\beta d\tau' \sum_{j,r} \underbrace{\int_0^\infty d\omega J(\omega) \left[ e^{-\omega|\tau-\tau'|} + 2n_B(\omega) \cosh \omega(\tau - \tau') \right]}_{B(\tau-\tau', x_j-x_r)} \cos \left( \omega \frac{x_j - x_r}{v_s} \right) \sigma_j(\tau) \sigma_r(\tau') \right\}, \quad (\text{A1})$$

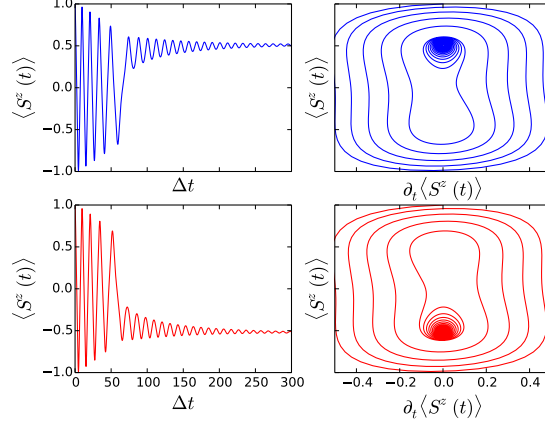


FIG. 8. Dissipative dynamics of the spin. The left panels represent the dynamics of  $\langle S^z(t) \rangle$  in the ferromagnetic phase, close to the transition point ( $K_r/K_c = 1.1$ ) for two different values of  $\alpha$ . The top panel corresponds to  $\alpha = 5.0 \times 10^{-3}$  while the bottom panel corresponds to  $\alpha = 5.5 \times 10^{-3}$ . On the right, we represent the phase portrait of the dynamics:  $\langle S^z(t) \rangle$  with respect to  $\partial_t \langle S^z(t) \rangle$ . Small fluctuations of the environment lead to different behaviours.

where  $n_B(\omega)$  is the Bose-Einstein distribution, the  $\sigma_j$  are the classical spin variables corresponding to the eigenvalues of the quantum operators  $\sigma_j^z$ , and  $\tau$  is the imaginary time. At zero temperature, we have

$$B(\tau - \tau', x_j - x_r) = \text{Re} \left[ \frac{2\pi\alpha\omega_c^2}{\left(1 + \omega_c|\tau - \tau'| + i\frac{x_j - x_r}{\xi}\right)^2} \right], \quad (\text{A2})$$

where  $\xi = v_s/\omega_c$ . On the other hand, the direct Ising coupling is responsible for a coupling term of the form

$$C(\tau - \tau', x_j - x_r) = \frac{K}{M} \delta(\tau - \tau'), \quad (\text{A3})$$

and the constant behavior in the space domain dominates in the low  $q$ , low  $\omega$  expansion of the action.

The mean-field coupling then dominates over the dissipative effects and we find back the characteristic features of the mean-field transition of the quantum Ising model in transverse field. This mean field behavior is valid as long as the direct Ising term  $K$  is *not* zero.

## Appendix B: Spin dynamics with the equations of motion

Here, we recover the mean-field spin dynamics thanks to the Heisenberg equations of motion, for a non-equilibrium initial state  $\prod_p |+_p, z\rangle$ . We reach the exact equation,

$$\begin{aligned} \dot{\sigma}_p^z = \int_{t_0}^t dt' & \left\{ \frac{-\Delta^2}{2} \left( \sigma_p^z(t') e^{-i\Omega_p(t')} e^{i\Omega_p(t)} + \sigma_p^z(t') e^{i\Omega_p(t')} e^{-i\Omega_p(t)} \right) \right. \\ & \left. + \Delta \sum_{j \neq p} K_{|j-p|}^r \left[ \sigma_j^z(t') \sigma_p^x(t') \cos \Omega_p(t) - \sigma_j^z(t') \sigma_p^y(t') \sin \Omega_p(t) \right] \right\}. \end{aligned} \quad (\text{B1})$$

Starting from a symmetric initial state, the time expectation value  $\langle \sigma_p^\nu(t) \rangle$  is independent of the site  $p$ , so that  $\langle \sigma_p^\nu(t) \rangle = \langle S^\nu(t) \rangle$  for all  $p$ , where  $S^\nu = 1/M \left( \sum_{p=1}^M \sigma_p^\nu \right)$  is a global spin operator. We derive then a mean-field weak-coupling equation of motion for  $\langle S^z(t) \rangle$  in the thermodynamic limit thanks to several approximations. First we assume that the time evolution of the bath operators is governed by the free bath Hamiltonian, and then we trace out the bosonic degrees of freedom in a weak coupling sense,

$$\langle \dot{S}^z(t) \rangle = -\Delta^2 \int_{t_0}^t dt' \langle S^z(t') \rangle \cos \left[ \frac{Q_1(t-t')}{\pi} \right] e^{-\frac{Q_2(t-t')}{\pi}} + \Delta_r K_r \int_{t_0}^t dt' \langle S^z(t') \rangle \langle S^x(t') \rangle. \quad (\text{B2})$$

We see in Fig. 8 that the presence of the Ising interaction together with the bath induces a rich dynamical behavior, and triggers a dynamical instability in the ferromagnetic phase close to the transition point. In this region, the differential equation shows the existence of two fixed attractive points, corresponding to the two degenerate ground states of the quantum Ising Hamiltonian. Starting from the non-equilibrium state  $\prod_p |_{+p,z}\rangle$ , the dynamics can relax to one of the two attractors, and small fluctuations of the value of  $\alpha$  may change the final point. Equation (B2) inherently contains some bi-stability features which are linked to the Ising term. For larger values of the Ising coupling, the energy barrier becomes too important for the spin to cross and the bistability is suppressed.

This bi-stability is independent from the nature of the bath, and still occurs when the noise becomes Markovian. The description of the dynamics through Lindblad terms for this mean field problem may lead to similar results.

- 
- [1] J.-M. Raimond, M. Brune and S. Haroche, Rev. Mod. Phys. **73**, 565 (2001).
  - [2] A. J. Leggett, S. Chakravarty, A. T. Dorsey, M. P. A. Fisher, A. Garg and W. Zwerger, Rev. Mod. Phys. **59**, 1 (1987).
  - [3] U. Weiss, Quantum dissipative systems, World Scientific, Singapore (2002).
  - [4] K. Le Hur, Annals of Physics **323** 2208-2240 (2008).
  - [5] A. O. Caldeira and A. J. Leggett, Physica 121A: 587 (1983).
  - [6] S. Jezouin, M. Albert, F. D. Parmentier, A. Anthore, U. Gennser, A. Cavanna, I. Safi and F. Pierre, Nat. Commun. **4**, 1802 (2013).
  - [7] H. T. Mebrahtu, I. V. Borzenets, D. E. Liu, H. Zheng, Y. V. Bomze, A. I. Smirnov, H. U. Baranger and G. Finkelstein, Nature **488**, p. 61 (2012).
  - [8] I. Safi and H. Saleur, Phys. Rev. Lett. **93**, 126602 (2004).
  - [9] K. Le Hur, Phys. Rev. Lett. **92**, 196804 (2004).
  - [10] P. G. de Gennes Solid State Commun. **1**, 132 (1963).
  - [11] P. Pfeuty, Annals of Physics **57**, 79-90 (1970).
  - [12] S. Sachdev, Quantum phase transitions, Cambridge University Press (1999).
  - [13] S. Pankov, S. Florens, A. Georges, G. Kotliar, and S. Sachdev, Phys. Rev. B **69**, 054426 (2004)
  - [14] S. Sachdev, P. Werner and M. Troyer, Phys. Rev. Lett. **92**, 237003 (2004).
  - [15] P. Werner, K. Volker, M. Troyer and S. Chakravarty, Phys. Rev. Lett. **94**, 047201 (2005).
  - [16] P. P. Orth, A. O. Imambekov and K. Le Hur, Phys. Rev. B **87**, 014305 (2013).
  - [17] P. P. Orth, A. O. Imambekov and K. Le Hur, Phys. Rev. A **82**, 032118 (2010).
  - [18] G. B. Lesovik, A. O. Lebedev and A. O. Imambekov, JETP Lett. **75**, 474 (2002).
  - [19] J. T. Stockburger and C. H. Mac, J. Chem. Phys. **110** (1999), 4983-4985.
  - [20] J. T. Stockburger and H. Grabert, Phys. Rev. Lett. **88**, 170407 (2002).
  - [21] J. T. Stockburger and H. Grabert, Chem. Phys. **296**, p. 159 (2004).
  - [22] A. Imambekov, V. Gritsev and E. Demler, Proceedings of the 2006 Enrico Fermi Summer School on "Ultracold Fermi gases", organized by M. Inguscio, W. Ketterle and C. Salomon (Varenna, Italy, June 2006) and arXiv:0703766.
  - [23] L. Henriot, Z. Ristivojevic, P. P. Orth and K. Le Hur, Phys. Rev. A **90**, 023820 (2014).
  - [24] R. Katz and P. B. Gossiaux, arXiv:1504.08087 (2015)
  - [25] J. Dalibard, I. Castin and K. Molmer, Phys. Rev. Lett. **68**, 580 (1992).
  - [26] R. Dum, P. Zoller, H. Ritsch, Phys. Rev. A **45**, 4879 (1992).
  - [27] I. Lesanovsky, M. van Horssen, M. Guta and J. P. Garrahan, Phys. Rev. Lett. **110**, 150401 (2013).
  - [28] G. Goldstein, C. Aron and C. Chamon, arXiv:1502.03046.
  - [29] P. Nalbach, S. Vishveshwara, and A. A. Clerk, arXiv:1503.06398.
  - [30] P. P. Orth, D. Roosen, W. Hofstetter and K. Le Hur, Phys. Rev. B **82**, 144423 (2010).
  - [31] R. Bulla, H.-J. Lee, N.-H. Tong and M. Vojta, Phys. Rev. B **71**, 045122 (2005).
  - [32] R. Bulla, T. A. Costi and T. Pruschke, Rev. Mod. Phys. **80**, 395 (2008).
  - [33] H. T. M. Nghiem and T. A. Costi, Phys. Rev. B **90**, 035129 (2014).
  - [34] M. Schiró, C. Joshi, M. Bordyuh, R. Fazio, J. Keeling, and H. E. Türeci, arXiv:1503.04456
  - [35] E. Sanchez-Burillo, D. Zueco, J. J. Garcia-Ripoll and L. Martin-Moreno, Phys. Rev. Lett. **113**, 263604 (2014).
  - [36] G. Kulaitis, F. Krüger, F. Nissen and J. Keeling, Phys. Rev. A **87**, 013840 (2013).
  - [37] Z. Ristivojevic, A. Petkovic, P. Le Doussal and T. Giamarchi, Phys. Rev. B **90**, 125144 (2014).
  - [38] T. Giamarchi and H. J. Schulz, Europhys. Lett. **3** 1287 (1987).
  - [39] F. Krzakala, A. Rosso, G. Semerjian, and F. Zamponi, Phys. Rev. B **78**, 134428 (2008).
  - [40] A. Friedenauer, H. Schmitz, J. T. Glueckert, D. Porras and T. Schaetz, Nat. Phys. **4**, 757 (2008).

- [41] R. Islam, E. Edwards, K. Kim, S. Korenblit, C. Noh, H. Carmichael, G.-D. Lin, L.-M. Duan, C.-C. J. Wang, J. Freericks, C. Monroe, *Nat. Commun.* **2**, 377 (2011).
- [42] A. Recati, P. O. Fedichev, W. Zwerger, J. von Delft and P. Zoller, *Phys. Rev. Lett.* **94**, 040404 (2005).
- [43] P. P. Orth and I. Stanic and K. Le Hur, *Phys. Rev. A* **77**, 051601(R) (2008).
- [44] R. Scelle, T. Rentrop, A. Trautmann, T. Schuster, and M. K. Oberthaler, *Phys. Rev. Lett.* **111**, 070401 (2013).
- [45] Y. R. P. Sortais, H. Marion, C. Tuchendler, A. M. Lance, M. Lamare, P. Fournet, C. Armellin, R. Mercier, G. Messin, A. Browaeys, and P. Grangier, *Phys. Rev. A* **75**, 013406 (2007).
- [46] L. Béguin, A. Vernier, R. Chicireanu, T. Lahaye, and A. Browaeys, *Phys. Rev. Lett.* **110**, 263201 (2013).
- [47] A. Grankin, E. Brion, E. Bimbard, R. Boddeda, I. Usmani, A. Ourjoumtsev and P. Grangier, *New J. Phys.* **16** 043020 (2014).
- [48] M. Marcuzzi, E. Levi, S. Diehl, J. P. Garrahan and I. Lesanovsky, *Phys. Rev. Lett.* **113**, 210401 (2014).
- [49] Y. O. Dudin, L. Li, F. Bariani and A. Kuzmich, *Nature Physics* **8**, 790-794 (2012)
- [50] M. Knap, A. Kantian, T. Giamarchi, I. Bloch, M. D. Lukin and E. Demler, *Phys. Rev. Lett.* **111**, 147205 (2013).
- [51] C. Sabin, A. White, L. Hackermuller and I. Fuentes, *Nature Scientific Reports*, Volume 4, id. 6436 (2014).
- [52] P. Calabrese, F. H. L. Essler, and M. Fagotti, *Phys. Rev. Lett.* **106**, 227203 (2011).
- [53] L. Foini, L. F. Cugliandolo and A. Gambassi, *J. Stat. Mech.* P09011 (2012).
- [54] A. Del Campo and W. H. Zurek, *Int. J. Mod. Phys. A* **29**, 1430018 (2014).
- [55] J-S Bernier, D. Poletti, P. Barmettler, G. Roux and C. Kollath, *Phys. Rev. A* **85**, 033641 (2012).
- [56] B. Sciolla and G. Biroli, *Phys. Rev. B* **88**, 201110(R) (2013).
- [57] A. Rancon, Chen-Lung Hung, Cheng Chin, and K. Levin *Phys. Rev. A* **88** 031601(R) (2013).
- [58] K. Sengupta, S. Powell and S. Sachdev, *Physical Review A* **69**, 5 (2004).
- [59] J. Dziarmaga, *Advances in Physics*, vol. **59**, issue 6, pp. 1063-1189 (2010).
- [60] C. De Grandi, A. Polkovnikov, “Quantum Quenching, Annealing and Computation”, Eds. A. Das, A. Chandra and B. K. Chakrabarti, *Lect. Notes in Phys.*, vol. 802 (Springer, Heidelberg 2010).
- [61] S. Diehl, A. Micheli, A. Kantian, B. Kraus, H.P. Büchler and P. Zoller, *Nature Physics* **4**, 878 (2008).
- [62] B. Kraus, S. Diehl, A. Micheli, A. Kantian, H.P. Büchler and P. Zoller, *Phys. Rev. A* **78**, 042307 (2008).
- [63] F. Verstraete, M. Wolf, I. Cirac, P. Zoller, *Nature Physics* **5**, 633 (2009).
- [64] D. P. S. McCutcheon, A. Nazir, S. Bose and A. J. Fisher, *Phys. Rev. B* **81**, 235321 (2010).
- [65] A. Dousse, L. Lanco, J. Suffczynski, E. Semenova, A. Miard, A. Lemaitre, I. Sagnes, C. Roblin, J. Bloch and P. Senellart, *Phys. Rev. Lett.* **101**, 267404 (2008).
- [66] J. M. Chow, J. M. Gambetta, Jens Koch, B. R. Johnson, J. A. Schreier, L. Frunzio, D. I. Schuster, A. A. Houck, A. Wallraff, A. Blais, M. H. Devoret, S. M. Girvin, and R. J. Schoelkopf, *Nature* **449**, 443-447 (2007).
- [67] M. R. Delbecq, L.E. Bruhat, J.J. Viennot, S. Datta, A. Cottet and T. Kontos *Nature Communications* **4**, 1400 (2013).
- [68] M. Garst, S. Kehrein, T. Pruschke, A. Rosch and M. Vojta, *Phys. Rev. B* **69**, 214413 (2004).
- [69] A. Winter and H. Rieger, *Phys. Rev. B* **90**, 224401 (2014)
- [70] L. Landau, *Physics of the Soviet Union* **2**, 46 (1932).
- [71] C. Zener, *Proc. R. Soc. of London A* **137**, 696 (1932).
- [72] E. C. G. Stueckelberg, *Helvetica Physica Acta* **5**, 369 (1932).
- [73] E. Majorana, *Nuovo Cimento* **9**, 43 (1932).
- [74] M. Wubs, K. Saito, S. Kohler, P. Hanggi and Y. Kayanuma, *Phys. Rev. Lett.* **97**, 200404 (2006).
- [75] K. Saito, M. Wubs, S. Kohler, Y. Kayanuma and P. Hanggi, *Phys. Rev. B* **75**, 214308 (2007).
- [76] R. P. Feynman and F. L. Vernon, *Ann. Phys. (N.Y.)* **24**, 118 (1963).
- [77] M. Schiro and M. Fabrizio, *Phys. Rev. B* **79**, 153302 (2009).
- [78] P. Werner, T. Oka, M. Eckstein and J. Millis, *Phys. Rev. B* **81**, 035108 (2010).
- [79] T. W. B. Kibble, *J. Phys. A* **9**, 1387 (1976); *Phys. Rep.* **67**, 183 (1980).
- [80] W. H. Zurek, *Nature (London)* **317**, 505 (1985); *Acta Phys. Pol. B* **24**, 1301 (1993); *Phys. Rep.* **276**, 177 (1996).
- [81] A. Del Campo and W. Zurek, *Int. J. Mod. Phys. A* **29**, 1430018 (2014).
- [82] B. Damski, *Phys. Rev. Lett.* **95**, 035701 (2005).
- [83] M. N. Kiselev, K. Kikoin and M. B. Kenmoe, *Europhys. Lett.* **104**, 57004 (2013).
- [84] S. N. Shevchenko, S. Ashhab and F. Nori, *Phys. Rept.* **492**, 1 (2010).
- [85] F. Anders, R. Bulla and M. Vojta, *Phys. Rev. Lett.* **98**, 210402 (2007).
- [86] K. Le Hur, Ph. Doucet-Beaupré and W. Hofstetter *Phys. Rev. Lett.* **99**, 126801 (2007).
- [87] C. Aron, M. Kulkarni and H. Tureci, arXiv:1412.8477.
- [88] L.-K. Lim, J.-N. Fuchs and G. Montambaux, *Phys. Rev. Lett.* **108**, 175303 (2012) and *Phys. Rev. Lett.* **112**, 155302 (2014).
- [89] J. Bauer, C. Salomon and E. Demler, *Phys. Rev. Lett.* **111**, 215304 (2013).